Visible Light Switchable Single-Chain Nanoparticles

Aidan E. Izuagbe, Vinh X. Truong, Bryan T. Tuten,* Peter W. Roesky,* and Christopher Barner-Kowollik*

ABSTRACT: We introduce a single-chain nanoparticle (SCNP) system, whose internal structure can be dynamically adjusted by two visible orthogonal colors of light ($\lambda_{1,\ max}$ = 620 and $\lambda_{2,\ max}$ = 415 nm). We construct linear polymer chains via nitroxide-mediated radical polymerization based on styrene building blocks, decorated with pendent phosphine ligands complexed with catalytically active gold motifs, and collapse the chain with variable amounts of photoresponsive visible light adaptive azobenzene units (13 and 23 mol %), enabling an in-particle *cis*/*trans* isomerization. The initial compaction due to the intramolecular cross-linking step is highly dependent on the number of cross-linking points in the initial chain and can reduce the hydrodynamic radius of the chains by up to approximately 44% for the highest azobenzene cross-linker density. The degree of post-folding reversible light-induced compaction is dependent on the number of azo-benzene units in the chain and is associated with a very clearly visible reversible change in UV absorptivity of the SCNP when switching irradiation wavelength. The reversible in-particle *cis*/*trans* isomerization is also well observable by ^{1}H NMR spectroscopy, indicating an in-particle light-induced polarity change. It is envisioned that the light-driven dynamically and reversibly altered particle core morphology and structure may find usage to reversibly restrict access into the SCNPs.

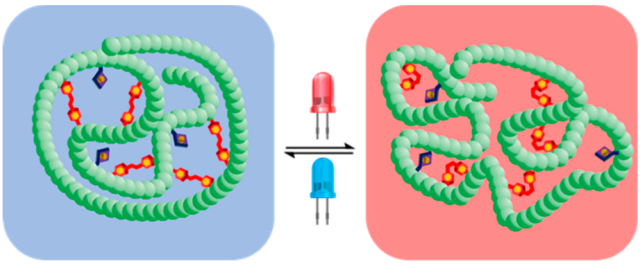

INTRODUCTION

The ability to fabricate small intramolecularly folded single-chain polymer nanoparticles (SCNPs), which can dynamically change their secondary and tertiary structure, is the next frontier in functional SCNP design. In addition to the perfectly defined and monodisperse primary structure of proteins or enzymes, their ability to fold or alter their tertiary structures is paramount to their function.[1−3] While perfect definition and monodispersity of the primary structure in synthetic polymers are still beset with considerable synthetic effort—especially in large quantities—controlling secondary and tertiary structure of SCNPs is within reach.[4−7]

Breaking ground in this field, Berda and co-workers first introduced stimuli responsive SCNPs capable of covalently folding and unfolding via disulfide bridges under oxidative or reductive conditions, respectively.[8] Similarly, our team exploited orthogonal host−guest chemistries to selectively fold and unfold structural segments of SCNPs with distinct chemical triggers.[9] These studies are among the early examples that describe dynamically changing tertiary structures of entire or parts of SCNPs, opening the door to dynamic folding possibilities including photochemical pathways,[10] dynamic covalent pathways,[11] strong secondary bonding pathways,[12] and others.[13,14] In addition, true tertiary structure manipulation has been introduced via irreversible secondary cross-linking reactions, for example, amine/anhydride cross-linking followed by thiol−ene chemistry, or Ugi and Passerini folding followed by hydrazino turn folding.[8,15]

Direct incorporation of photoswitches into moieties used to cross-link SCNPs is an enticing strategy toward the dynamic manipulation of the tertiary structure of SCNPs. Specifically, various photoswitching motifs, including azobenzene, coumarin, spiropyran, and diarylethene, have been incorporated into complex polymer architectures to obtain morphological control.[16−19] By far the most well-known and utilized photoswitches are bisimines and azobenzenes.[20−23] With their ease of synthesis and ability to adjust their switching wavelengths,[24,25] azobenzenes fused with the power of spatio-temporal control of photochemistry constitute ideal platforms to manipulate the tertiary structure of SCNPs. As of now, few examples exist where photoswitches are directly incorporated into SCNPs as the cross-linked bridges, typically relegated to side-chain modifications.[26−29]

Dynamic tertiary (and secondary) changes to proteins and enzymes equip them with the ability to manipulate the rates, in which they drive biochemical processes.[3] While biological

Scheme 1. Illustration of the Concept of Photo-Reversibly Foldable Potential Catalytic SCNPs; (a) (i) Linear Polymer Bearing [Ar_3PAuCl] as a Potential Catalytic Site; (ii) Compaction of the Linear Polymer into an SCNP Using an External Azobenzene Cross-Linkers; (iii) Reversible Light-Induced Switching of the Azobenzene Cross-Links Alters the SCNP Morphology; (iv) Azobenzene Isomerization Restricts Access to the Gold Catalyst; (v) SCNP is Recycled and Utilized in Further Catalytic Cycles. (b) Simplified Synthetic Overview Towards Photo-Reversibly Foldable Catalytic SCNPs. (c) *Ortho*-Tetra Chlorinated Azobenzenes Used to Cross-Link the SCNP, Irradiation with Two Orthogonal Wavelengths of Light Inducing *Cis*/*Trans* Isomerization and Morphological Changes within the SCNP, Triaryl Phosphine is Functionalized with an Au(I) Center Constituting the Catalytic Site of the SCNP. (d) *Cis*/*Trans* Switching of the SCNP Using $\lambda_{1,\,max}$ = 620 nm and $\lambda_{2,\,max}$ = 415 nm

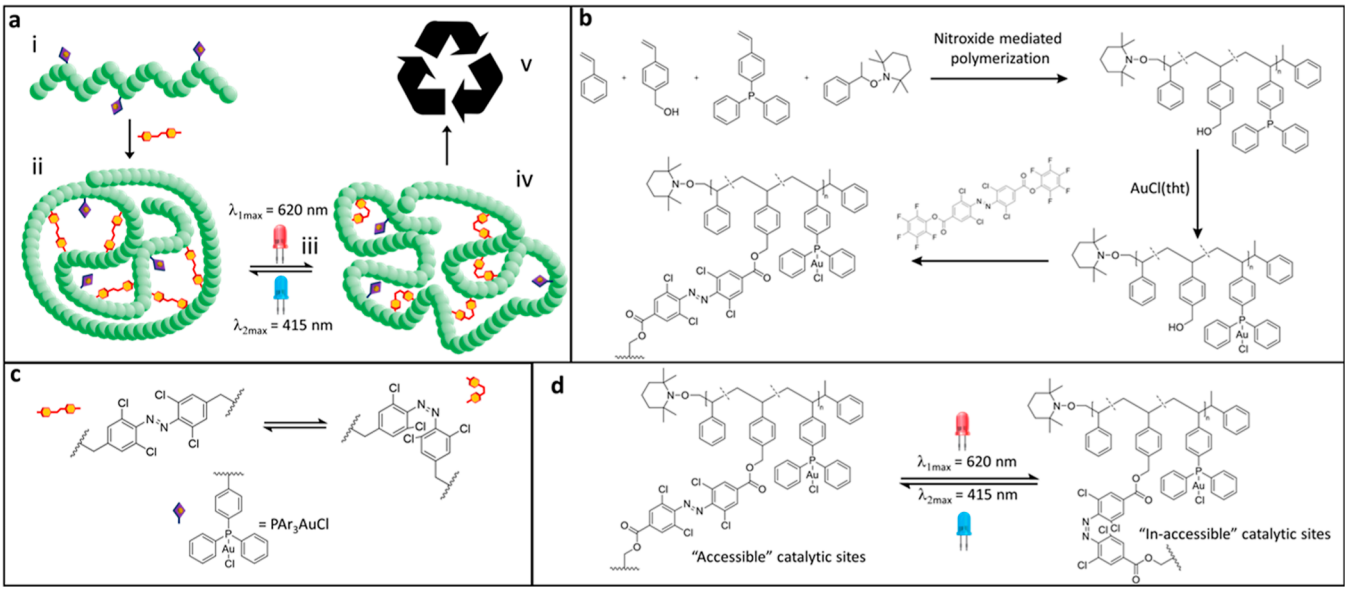

systems require precise secondary bonding interactions to decrease activation barriers, synthetic systems often turn to organometallic entities. Some classic examples include the use of palladium in Suzuki couplings,[30] ruthenium in metathesis reactions,[31] rhodium-based complexes such as the Wilkinson catalyst for hydrogenation reactions,[32] and iridium in the dehydrogenation of alkanes.[33] A further interesting reaction is the metal-catalyzed hydroamination of alkenes and alkynes.[34,35] The direct addition of a nitrogen to a carbon atom facilitated by a phosphine-gold-catalyzed hydroamination affords a mild and atom efficient method of accessing industrially relevant nitrogen containing compounds.[35] Hydroamination of an alkyne has been achieved using an SCNP bearing a phosphine-gold pendant group,[36] highlighting the compatibility of hydroamination with an SCNP environment.[37]

Herein, we introduce a class of SCNPs, whose internal morphology and thus degree of compaction—and more critically internal molecular configuration—can be photodynamically adapted.[38] We design our macromolecular constructs on the basis of a robust polystyrene chain, decorated with gold-complexed phosphine ligands and cross-linked with visible light reversibly switchable tetrachloro-substituted azobenzene units ($\lambda_{1,\,max}$ = 620 nm and $\lambda_{2,\,max}$ = 415 nm) (refer to Scheme 1). These metal complex carrying entities are shown to be reversibly and robustly switchable entirely with orthogonal wavelengths of visible light without hysteresis.

RESULTS AND DISCUSSION

Linear Polymer Design. Initially, we construct two linear copolymers via nitroxide-mediated polymerization[39] consisting of a styrene backbone-bearing pendant groups that will either facilitate intramolecular cross-linking into the SCNP or act as a coordinating ligand for a gold unit. Specifically, styrene was copolymerized with vinyl benzyl alcohol and a styrene-based derivative of triphenylphosphine to generate statistical copolymers that differ from each other on their benzyl alcohol content (Table 1). The polymers possess approximately the same triarylphosphine content (Ar_3P, between 6 and 7 mol %) as evidenced by ^{1}H NMR spectroscopy (refer to Section 4 in Supporting Information for polymer composition calculations). The triarylphosphine pendant moieties enable the subsequent attachment of catalytically active gold units, while protecting the triarylphosphine from oxidation.

Table 1. Composition Characteristics of the Hydroxy and Gold-Functionalized Polymers[a]

polymer	mol % OH (%)	mol % Ar_3PAuCl (%)	M_n/g mol−1
Au-P-13	13	7	21,000
Au-P-23	23	6	26,000

[a]Molecular weights reported are relative to a poly(styrene) calibration.

Coordination of [(tht)AuCl] (tht = tetrahydrothiophene) to the phosphine ligands of the linear polymers forming the [Ar_3PAuCl] complex was confirmed by $^{31}P\{^1H\}$ NMR spectroscopy (Figures S26, and S29). An unambiguous shift of the free phosphine resonances (δ = −6 ppm) downfield (δ = 31 ppm) is observed upon complexation. ^{1}H NMR spectroscopy indicates an increase in the intensity of the triarylphosphine-associated resonance (at δ = 7.31 ppm), attributed to the successful coordination of the gold-functionalized linear polymers. An increase in the number average molecular weight of all the linear polymers is concomitantly observed (Figures S27 and S30), associated with the

coordination of the gold atoms to the triarylphosphine pendant groups.

Synthesis and Characterization of the SCNP. SCNPs can be formed via the introduction of an external cross-linking agent to a linear polymer, which upon coupling to suitable polymeric functional groups induces intramolecular cross-linking into an SCNP.[5] To equip an SCNP with reversible compatibility/in-particle morphological change, we employ an external cross-linking agent, that is, *ortho*-tetra chlorinated azobenzene (***o*-AzoCl$_4$**) functionalized at the 4′4 positions with pentafluorphenyl esters (**PFP**) to enable cross-linking. Light-induced *cis* and *trans* isomerization of the ***o*-AzoCl$_4$** cross-links allows for access to a photo reversible method of altering the internal morphology of the SCNP. Utilizing ***o*-AzoCl$_4$** as cross-links as opposed to backbone functionalities is synthetically less intensive, while affording light-induced structural control over the SCNP. Free alcohol pendant groups on the linear polymer precursor serve to intramolecularly collapse the polymer into an SCNP via the dimethyl aminopyridine-catalyzed esterification between **PFP** ester decorated ***o*-AzoCl$_4$** and the pendant alcohol groups. Critically, tetra-chlorination at the *ortho* positions of the aromatic system affords a *cis* isomer that can be generated using irradiation with $\lambda_{1,max}$ = 620 nm initially demonstrated in a small molecule study herein (Figure S43). *Trans* reversion is achieved by irradiation with $\lambda_{2,max}$ = 415 nm light, and thermal reversion into the *trans* isomer remains minimal after 16 h, indicating a thermally stable *cis* isomer (refer to Section 7.6 for the thermal stability and Section 7.7 for LED emission spectra of Supporting Information). The long thermal half-life is a result of a low-energy n-orbital facilitated by the electron withdrawing nature of *ortho*-chlorination.[24,40] A long-lived thermal half-life of the *cis* isomer within the SCNP provides a critical advantage compared to conventional azobenzenes, to ensure that—when irradiated—the SCNP remains in its switched configuration. Compaction into an SCNP is typically conducted under high polymer dilution concentrations (<1 mg mL^{-1}) with an excess of cross-linking agents.[41] Cross-linking is achieved using a continuous addition method, adding a dilute solution of the gold-functionalized polymers **Au-P** to a concentrated solution of the ***o*-AzoCl$_4$PFP** cross-linker (refer to Section 5 in the Supporting Information for SCNP synthesis).

The folded state of the SCNPs was confirmed via size exclusion chromatography (Figure 1) using tetrahydrofuran (THF) as the eluent. Longer retention times for the SCNPs are observed when compared to their linear counter parts. Apparent number average molecular weights of 21,000 and 26,000 g mol^{-1} were observed for the two linear polymers **Au-P-13** and **Au-P-23**, respectively. SCNPs generated from the two precursors polymers bearing 23 mol % OH (**Azo-Au SCNP-23**) and 13 mol % OH (**Azo-Au-SCNP-13**) displayed apparent number average molecular weights of 14,000 and 16,000 g mol^{-1}, respectively. This corresponds to a compaction of 24% for **Azo-Au-SCNP-13** and 46% for **Azo-Au-SCNP-23**. It was observed that by increasing the amount of the pendant alcohol content in the polymer, the observed compaction also increased. To confirm that the ***o*-AzoCl$_4$** units are responsible for the intramolecular cross-linking and thus compaction, the SEC (refractive index) trace is overlayed with the extracted Size Exclusion Chromatography (SEC) UV−vis trace. Both the UV−vis and Refractive Index (RI) traces coincide (Figure S33). Furthermore, the intensity of the UV−vis signal when compared to the RI signals indicates the presence of the strongly absorbing azobenzene cross-link (Figure S33). ^{1}H NMR spectroscopy was further employed to track the formation of the SCNPs (Figures S31 and S34). A clear down-field shift of the resonances associated with the benzylic alcohol pendant groups (δ = 4.5 ppm) of the linear polymers is observed as they are converted to benzylic esters (δ = 5.3 ppm). Furthermore, a broad resonance (δ = 8.1 ppm) associated with the symmetrical azobenzene aromatic hydrogens in the α-position to the ester functionality is observed. Diffusion coefficients of the parent and compacted polymer system were determined via diffusion ordered spectroscopy (DOSY) measurements (in $CDCl_3$) for **Azo-Au-SCNPs**, revealing a hydrodynamic diameter of 1.68 nm for the **Azo-Au-SCNP-13** and 2.59 nm for the parent polymer **Au-P-13**, indicating a 35% decrease in hydrodynamic diameter. **Azo-Au-SCNP-23** coincidentally also displayed a hydrodynamic diameter of 1.68 and 2.99 nm for the parent polymer representing a reduction in diameter of 44% (refer to Section 7.8 of Supporting Information for DOSY data). The *trans* configuration of ***o*-AzoCl$_4$** displays a distinct band in the UV region associated with a symmetry allowed $\pi-\pi^*$ transition. Upon irradiation with $\lambda_{1,max}$ = 620 nm, the intensity of this band decreases, and the symmetry forbidden $n-\pi^*$ transition in the visible region increases with increasing irradiation and *cis* isomer content. These two transitions allow for accurate determination of the spectral properties of **Azo-Au-SCNP** via UV−vis spectrometry. The successful collapse into the SCNP via the visible light active azobenzene cross-linker is highlighted by the presence of the $n-\pi^*$ band in the visible region with a λ_{max} of 440 nm (Figure 2a). A small molecule model consisting of the tetra chlorinated azobenzene diacid displays a distinct $n-\pi^*$ transition at 440 nm, closely matching that seen for **Azo-Au-SCNP-13** (Figure S43). The hydroamination between amines and electron-deficient unsaturated C=C bonds was employed to establish the catalytic ability of the **Azo-Au-SCNPs** utilizing **Azo-Au-SCNP-13** as an exemplar system in some preliminary studies (refer to Section 6 in Supporting Information section). It is well known that [Ph_3PAuCl] is able to catalyze hydroamination reactions via

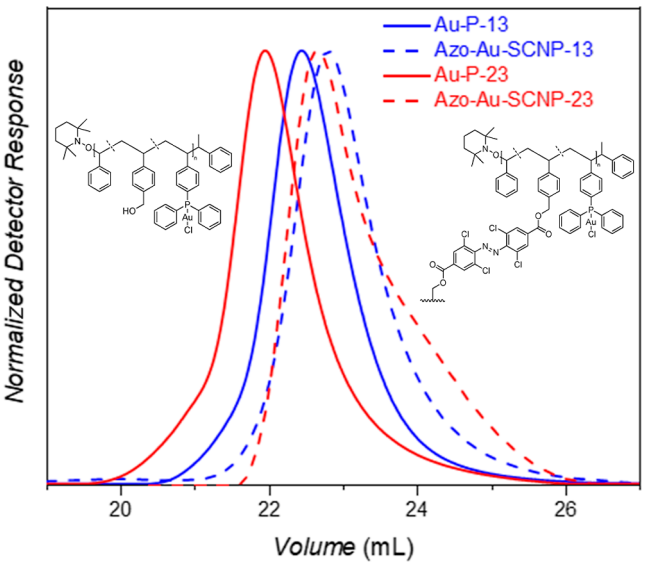

Figure 1. Compaction of linear polymers into **Azo-Au-SCNPs** followed via SEC as a shift toward longer retention times.

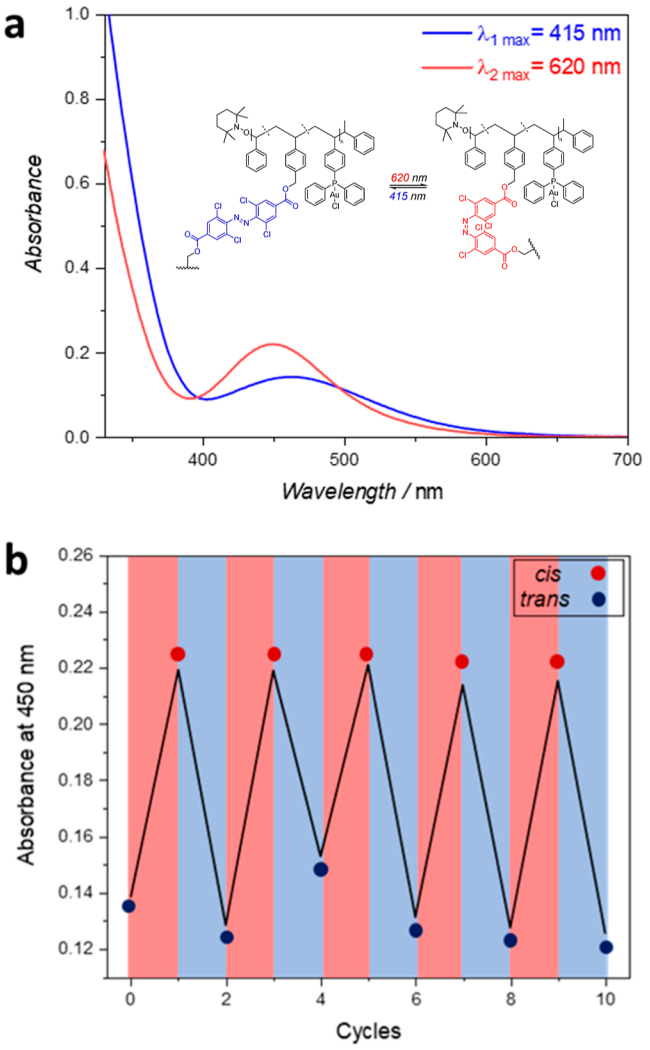

Figure 2. (a) UV−vis analysis depicting the increase in the absorption of the 440 nm $n-\pi^*$ visible band upon irradiation of **Azo-Au-SCNP-13** with $\lambda_{1,max}$ = 620 nm light. No change in absorption occurs after 1 h of continuous irradiation. Irradiation with $\lambda_{2,max}$ = 415 nm light results in reversion of the 440 nm band after 30 min of irradiation. (b) Photoswitching fatigue experiment of **Azo-Au-SCNP-13** using alternating irradiation with $\lambda_{1,max}$ = 620 nm and $\lambda_{2,max}$ = 415 nm.

cationic activation with a suitable co-catalyst.[36,42] The catalytic active species is a cation of $[Ph_3PAu]^+$, which is generated by chloride abstraction via a co-catalyst. Here, we employ $[Zn(OTF)_2]$ as a co-catalyst to activate the polymer bound $[Ar_3PAuCl]$ complex. **Azo-Au-SCNP-13** activated by $[Zn(OTF)_2]$ was able to catalyze the intramolecular hydroamination of a substrate bearing an internal alkyne and primary amine into a ring-closed product. Additionally, a control experiment with only the co-catalyst was carried out, where $[Zn(OTF)_2]$ and the substrate are present in the reaction mixture. As expected, this test showed no undesired catalysis between the co-catalyst, $[Zn(OTF)_2]$, and the substrate under the applied conditions.

Photoresponsivity. Collapse of the linear polymers into the **Azo-Au-SCNPs** affords a particle with reversibly switchable cross-links addressable with orthogonal wavelengths of light. The photoresponsivity of the SCNPs is investigated using **Azo-Au-SCNP-13** as the model system upon irradiation with the two orthogonal wavelengths used to reversibly isomerize the ***o*-AzoCl$_4$** cross-links. UV−vis was used to monitor the absorption spectra of **Azo-Au-SCNP-13** upon irradiation with $\lambda_{1\ max}$ = 620 nm into the *cis* configuration and λ_{2max} = 415 nm light into the *trans-* configuration.

Irradiation with $\lambda_{1,max}$ = 620 nm light results in a clear increase in the absorption of the visible light band at 440 nm. This absorption band is attributed to the $n-\pi^*$ transition of the ***o*-AzoCl$_4$***cis* isomer (Figure 2a). An increase in absorption indicates an increasing *cis* isomer content in the SCNP. After 1 h of irradiation, no further increase in the visible band is observed. Irradiation with $\lambda_{2\ max}$ = 415 nm light results in a decrease in the absorption of the visible light band (440 nm). After 30 min of continuous irradiation with λ_2, the *trans* isomer content in the SCNP is restored to its initial level prior to $\lambda_{1,\ max}$ = 620 nm irradiation. To ensure that the photodynamic SCNP system is photoswitchable without hysteresis, **Azo-Au-SCNP-13** was subjected to five cycles of alternating λ_1 and λ_2 irradiation (Figure 2b). The absorption profiles of both the *cis* and *trans* isomers were retained throughout the cycles, indicating a conserved switching mechanism.

Azobenzene isomers display substantially different electronic properties when switching from the *trans* isomer to the *cis* isomer, which are reflected in the ^{1}H NMR spectrum of the SCNPs after exposure to the two colors of visible light. Isomerization can be tracked using the difference in alignment of the electron cloud between *cis* and *trans* isomers of the aromatic ring. Such an alignment gives rise to an anisotropic effect that shifts all aromatic proton resonances within the azobenzene moiety as a function of the prevailing isomer.[43] In the *cis* isomer form, the aromatic proton resonances are observed up field in comparison to the corresponding*trans* isomer resonances.

The *trans* isomer of the ***o*-AzoCl$_4$** cross-links within the **Azo-Au-SCNP-13** displays aromatic proton resonances at (δ = 8.1 ppm). Upon irradiation of the **Azo-Au-SCNP-13** with λ_1, these protons shift up field to (δ = 7.8 ppm), indicating isomerization into the *cis* isomer. Integration of these two resonances after 1 h of irradiation reveals a *cis*/*trans* ratio of 7:3 (Figure 3). Furthermore, the *cis* isomer appears to isomerize very slowly, as observed in the thermal relaxation studies

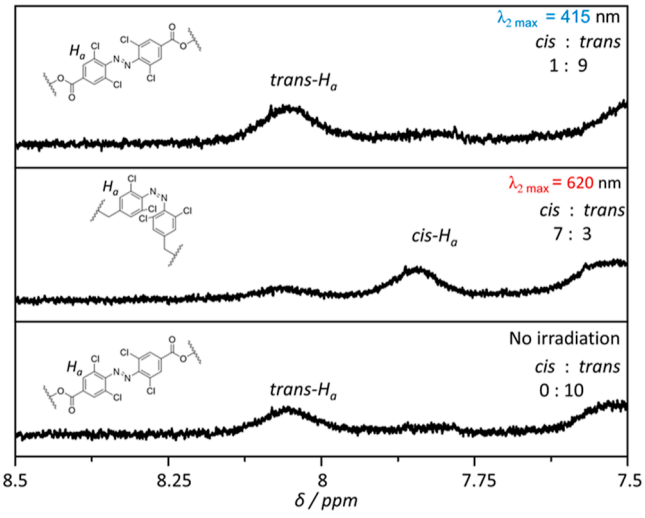

Figure 3. ^{1}H NMR spectra tracing the photodynamic switching of **Azo-Au-SCNP-13** compacted via ***o*-AzoCl$_4$** cross-links upon $\lambda_{1,\ max}$ = 620 nm and $\lambda_{2,\ max}$ = 415 nm irradiation.

(Figure S48). Irradiation with λ_2 results in the restoration of the *trans* isomer after 30 min of irradiation, indicating successful switching of the azobenzene cross-links. Switching the ***o*-AzoCl$_4$** cross-links from *trans* to *cis* was expected to result in some limited compaction of the **Azo-Au-SCNPs**, visible in chromatograms as an increase in retention volume. Thus, the effect of irradiation of the **SCNPs** with $\lambda_{1,\,max}$ = 620 nm and $\lambda_{2,\,max}$ = 415 nm light is followed independently with SEC analysis.

Upon irradiation with $\lambda_{1,\,max}$ = 620 nm light, **Azo-Au-SCNP-13** displayed a slight compaction indicated by an increase in retention volume (Figure 4, red trace), corresponding to an—

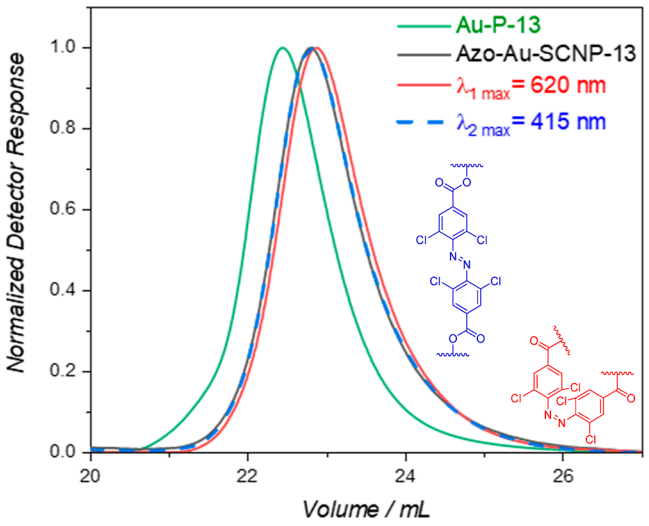

Figure 4. SEC analysis of the linear polymer (**Au-P-13**) (green), compaction into the SCNP (**Azo-Au-SCNP-13**) (black) followed by irradiation with $\lambda_{1,\,max}$ = 620 nm light (red) and subsequent irradiation with $\lambda_{2,\,max}$ = 415 nm light (blue dotted).

apparent—small change in the number average molecular weight. Irradiation of **Azo-Au-SCNP-13** with $\lambda_{2,\,max}$ = 415 nm reverts the observed compaction to afford an SEC trace (Figure 4, blue trace) in alignment with the initial non-irradiated SEC trace (Figure 4, black trace). A slight difference in SEC chromatograms was observed for the different benzyl alcohol compositions of **Azo-Au-SCNP-23** and **Azo-Au-SCNP-13** (refer to Figure S46 for **Azo-Au-SCNP-23** SEC data). Triplicates of this experiment with **Azo-Au-SCNP-13** were completed to confirm that the compaction is statistically significant (Figure S44). Peak molecular weight (M_p) values were used to highlight the retention time shifts in the polymer distributions. The M_p values established from the triplicate experiments were tabulated and averaged, indicating a shift in M_p of close to 1000 g mol^{-1} to an apparent lower molecular weight upon irradiation with $\lambda_{1,\,max}$ = 620 nm light. Subsequent irradiation with $\lambda_{2,\,max}$ = 415 nm light resulted in a close to 900 g mol^{-1} reversion to higher apparent molecular weights, closely matching the initial SCNP (Figure S45). It was envisioned that as the hydroxy and thus azobenzene content increased, the $\lambda_{1,\,max}$ = 620 nm light-induced compaction of the SCNPs would also increase. **Azo-Au-SCNP-13** displayed a more pronounced light-induced compaction (6%) than **Azo-Au-SCNP-23** (3%). The increased cross-linking density of **Azo-Au-SCNP-23** may diminish the effect of azobenzene switching due to the more constrained polymeric environment and subsequent restriction of movement available to the formed SCNP. The small shift to longer retention times can be attributed to the change in end-to-end length of the azobenzene cross-links as they switch from *trans* (9.9 Å) to *cis* isomers (5.5 Å).[44] Accompanying the change in the end-to-end length of the ***o*-AzoCl$_4$** cross-links is a change in the net dipole moment from 0 D to 3 D,[45] *trans* to *cis*. It is reasonable to assume that due to this change in polarity in solvents such as THF, the overall particles hydrodynamic radius would likely increase due to the enhanced solvation. Observation of a shift to shorter retention times, albeit small, is indicative of a more substantive compaction mechanism. With varying solvent conditions, this compaction may vary. Such a solvent-dependent mechanism is of key interest for catalytic processes, particularly those that are required or can be conducted in apolar solvents. DOSY spectra were considered as a method of monitoring the light-induced contraction and expansion of the **Azo-Au-SCNPs**. Due to the relatively small shift observed post $\lambda_{1,\,max}$ = 620 nm irradiation, it was determined that DOSY techniques would not be able to resolve the difference between the open and closed form of the **Azo-Au-SCNPs**.

CONCLUSIONS

In the current contribution, we introduce an advanced SCNP system, where compaction and polarity can be switched by two disparate colors of visible light ($\lambda_{1,\,max}$ = 620 nm and $\lambda_{2,\,max}$ 415 nm). We achieve the light adaptable nature of the SCNPs by introducing visible light responsive azobenzene units as the cross-linking moieties. The SCNP system is based on a polystyrene backbone prepared via nitroxide-mediated polymerization, featuring pendent phosphine and hydroxy functionalities, which are, respectively, used for metal loading (Au) and cross-linking. Evidenced by DOSY, we observe a maximum compaction degree of up to 44%, based on an overall molecular weight of 26,000 g mol^{-1}of the parent polymer, featuring a molar fraction of the functional groups of 12:4:1 (styrene/OH/phosphine). The visible light-induced reversible compaction of the SCNP systems was evidenced via a small shift toward higher retention times. Critically, however, the reversible inner SCNP morphological change was underpinned by ^{1}H NMR spectroscopy, allowing to directly map the number of *cis* versus *trans* configured azobenzene units after irradiation with the respective visible light color. UV−vis spectroscopy further confirmed the hysteresis free switching mechanism of the SCNPs via changes in the absorption profiles of the *cis* and *trans* isomers. A maximum of 70% of the azobenzene units within the SCNP can be reversibly switched, with no hysteresis observed over five switching cycles. Furthermore, our SCNP system is decorated with catalytically active Au-complexes able to catalyze the intramolecular hydroamination of an alkyne and amine. We envision in future work that access to these units may be controlled by the color of light the SCNP system is exposed to, thus enabling control of catalysis through morphological control within the SCNP internal architecture. We submit that the current findings constitute a step-change in reversible and remotely driven control over SCNP geometry, potentially constituting an entry point into controlling thermally driven catalytic processes with light.

ASSOCIATED CONTENT

Supporting Information

The Supporting Information is available free of charge at https://pubs.acs.org/doi/10.1021/acs.macromol.2c01467.

Full experimental details, synthesis/characterization of polymers, monomers and SCNPs, substrate synthesis, catalytic experiments, and primary DOSY data (PDF)

AUTHOR INFORMATION

Corresponding Authors

Bryan T. Tuten − *Centre for Materials Science, Queensland University of Technology, Brisbane, Queensland 4000, Australia; School of Chemistry and Physics, Queensland University of Technology, Brisbane, Queensland 4000, Australia;* orcid.org/0000-0002-5419-7561; Email: bryan.tuten@qut.edu.au

Peter W. Roesky − *Institute of Inorganic Chemistry, Karlsruhe Institute of Technology (KIT), 76131 Karlsruhe, Germany;* orcid.org/0000-0002-0915-3893; Email: roesky@kit.edu

Christopher Barner-Kowollik − *Centre for Materials Science, Queensland University of Technology, Brisbane, Queensland 4000, Australia; School of Chemistry and Physics, Queensland University of Technology, Brisbane, Queensland 4000, Australia; Institute of Nanotechnology (INT), Karlsruhe Institute of Technology (KIT), 76344 Eggenstein-Leopoldshafen, Germany;* orcid.org/0000-0002-6745-0570; Email: christopher.barner-kowollik@kit.edu, christopher.barnerkowollik@qut.edu.au

Authors

Aidan E. Izuagbe − *Centre for Materials Science, Queensland University of Technology, Brisbane, Queensland 4000, Australia; School of Chemistry and Physics, Queensland University of Technology, Brisbane, Queensland 4000, Australia; Institute of Inorganic Chemistry, Karlsruhe Institute of Technology (KIT), 76131 Karlsruhe, Germany*

Vinh X. Truong − *Centre for Materials Science, Queensland University of Technology, Brisbane, Queensland 4000, Australia; School of Chemistry and Physics, Queensland University of Technology, Brisbane, Queensland 4000, Australia;* orcid.org/0000-0001-5553-6097

Complete contact information is available at: https://pubs.acs.org/10.1021/acs.macromol.2c01467

Notes

The authors declare no competing financial interest.

ACKNOWLEDGMENTS

C.B.K. acknowledges funding from the Australian Research Council (ARC) in the form of a Laureate Fellowship (FL170100014) enabling his photochemical research program as well as continued key support from the Queensland University of Technology (QUT). B.T.T. acknowledges the ARC for funding in the context of a DECRA Fellowship. A.E.I. is grateful for a PhD scholarship from the Queensland University of Technology (QUT). P.W.R. acknowledges KIT for funding.

REFERENCES

(1) Breslow, R. Biomimetic Chemistry and Artificial Enzymes: Catalysis by Design. *Acc. Chem. Res.* **1995**, *28*, 146−153.

(2) Guzman, I.; Gruebele, M. Protein Folding Dynamics in the Cell. *J. Phys. Chem. B* **2014**, *118*, 8459−8470.

(3) Mitrea, D. M.; Kriwacki, R. W. Regulated Unfolding of Proteins in Signaling. *FEBS Lett.* **2013**, *587*, 1081−1088.

(4) Hanlon, A. M.; Lyon, C. K.; Berda, E. B. What Is Next in Single-Chain Nanoparticles? *Macromolecules* **2016**, *49*, 2−14.

(5) Lyon, C. K.; Prasher, A.; Hanlon, A. M.; Tuten, B. T.; Tooley, C. A.; Frank, P. G.; Berda, E. B. A brief user's guide to single-chain nanoparticles. *Polym. Chem.* **2015**, *6*, 181−197.

(6) Lutz, L.; Ouchi, O.; Liu, R.; Sawamoto, S. Sequence-Controlled Polymers. *Science* **2013**, *341*, 1238149.

(7) Austin, M. J.; Rosales, A. M. Tunable Biomaterials from Synthetic, Sequence-Controlled Polymers. *Biomater. Sci.* **2019**, *7*, 490−505.

(8) Tuten, B. T.; Chao, D.; Lyon, C. K.; Berda, E. B. Single-Chain Polymer Nanoparticles via Reversible Disulfide Bridges. *Polym. Chem.* **2012**, *3*, 3068−3071.

(9) Fischer, T. S.; Schulze-Sünninghausen, D.; Luy, B.; Altintas, O.; Barner-Kowollik, C. Stepwise Unfolding of Single-Chain Nanoparticles by Chemically Triggered Gates. *Angew. Chem.* **2016**, *55*, 11276−11280.

(10) Frisch, H.; Bloesser, F. R.; Barner-Kowollik, C. Controlling Chain Coupling and Single-Chain Ligation by Two Colours of Visible Light. *Angew. Chem.* **2019**, *58*, 3604−3609.

(11) Whitaker, D. E.; Mahon, C. S.; Fulton, D. A. Thermoresponsive Dynamic Covalent Single-Chain Polymer Nanoparticles Reversibly Transform into a Hydrogel. *Angew. Chem.* **2013**, *52*, 956−959.

(12) Yilmaz, G.; Uzunova, V.; Napier, R.; Becer, C. R. Single-Chain Glycopolymer Folding via Host−Guest Interactions and Its Unprecedented Effect on DC-SIGN Binding. *Biomacromolecules* **2018**, *19*, 3040−3047.

(13) Hosono, N.; Kushner, A. M.; Chung, J.; Palmans, A. R. A.; Guan, Z.; Meijer, E. W. Forced Unfolding of Single-Chain Polymeric Nanoparticles. *J. Am. Chem. Soc.* **2015**, *137*, 6880−6888.

(14) Kodura, D.; Houck, H. A.; Bloesser, F. R.; Goldmann, A. S.; Du Prez, F. E.; Frisch, H.; Barner-Kowollik, C. Light-Fueled Dynamic Covalent Crosslinking of Single Polymer Chains in Non-Equilibrium States. *Chem. Sci.* **2021**, *12*, 1302−1310.

(15) Cole, J. P.; Lessard, J. J.; Rodriguez, K. J.; Hanlon, A. M.; Reville, E. K.; Mancinelli, J. P.; Berda, E. B. Single-Chain Nanoparticles Containing Sequence-Defined Segments: Using Primary Structure Control to Promote Secondary and Tertiary Structures in Synthetic Protein Mimics. *Polym. Chem.* **2017**, *8*, 5829−5835.

(16) Gao, Y.; Guo, R.; Feng, Y.; Zhang, L.; Wang, C.; Song, J.; Jiao, T.; Zhou, J.; Peng, Q. Self-Assembled Hydrogels Based on Poly-Cyclodextrin and Poly-Azobenzene Compounds and Applications for Highly Efficient Removal of Bisphenol A and Methylene Blue. *ACS Omega* **2018**, *3*, 11663−11672.

(17) Chen, Q.; Yang, Q.; Gao, P.; Chi, B.; Nie, J.; He, Y. Photopolymerization of Coumarin-Containing Reversible Photoresponsive Materials Based on Wavelength Selectivity. *Ind. Eng. Chem. Res.* **2019**, *58*, 2970−2975.

(18) ter Schiphorst, J.; van den Broek, M.; de Koning, T.; Murphy, J. N.; Schenning, A. P. H. J.; Esteves, A. C. C. Dual Light and Temperature Responsive Cotton Fabric Functionalized with a Surface-Grafted Spiropyran−NIPAAm-Hydrogel. *J. Mater. Chem. A* **2016**, *4*, 8676−8681.

(19) Shimizu, K.; Métivier, R.; Kobatake, S. Synthesis and Fluorescence on/off Switching of Hyperbranched Polymers Having Diarylethene at the Branching Point. *J. Photochem. Photobiol., A* **2020**, *390*, 112341.

(20) Shin, J.; Sung, J.; Kang, M.; Xie, X.; Lee, B.; Lee, K. M.; White, T. J.; Leal, C.; Sottos, N. R.; Braun, P. V.; Cahill, D. G. Light-Triggered Thermal Conductivity Switching in Azobenzene Polymers. *Proc. Natl. Acad. Sci. U.S.A.* **2019**, *116*, 5973.

(21) Zhou, Y.; Chen, M.; Ban, Q.; Zhang, Z.; Shuang, S.; Koynov, K.; Butt, H.-J.; Kong, J.; Wu, S. Light-Switchable Polymer Adhesive Based on Photoinduced Reversible Solid-to-Liquid Transitions. *ACS Macro Lett.* **2019**, *8*, 968−972.

(22) Kuenstler, A. S.; Clark, K. D.; Read de Alaniz, J.; Hayward, R. C. Reversible Actuation via Photoisomerization-Induced Melting of a

Semicrystalline Poly(Azobenzene). *ACS Macro Lett.* **2020**, *9*, 902−909.
(23) Li, L.; Li, Y.; Wang, S.; Ye, L.; Zhang, W.; Zhou, N.; Zhang, Z.; Zhu, X. Morphological Modulation of Azobenzene-Containing Tubular Polymersomes. *Polym. Chem.* **2021**, *12*, 3052−3059.
(24) Konrad, D. B.; Savasci, G.; Allmendinger, L.; Trauner, D.; Ochsenfeld, C.; Ali, A. M. Computational Design and Synthesis of a Deeply Red-Shifted and Bistable Azobenzene. *J. Am. Chem. Soc.* **2020**, *142*, 6538−6547.
(25) Merino, E. Synthesis of Azobenzenes: The Coloured Pieces of Molecular Materials. *Chem. Soc. Rev.* **2011**, *40*, 3835−3853.
(26) Wen, W.; Chen, A. The Self-Assembly of Single Chain Janus Nanoparticles from Azobenzene-Containing Block Copolymers and Reversible Photoinduced Morphology Transitions. *Polym. Chem.* **2021**, *12*, 2447−2456.
(27) Fan, W.; Tong, X.; Li, G.; Zhao, Y. Photoresponsive Liquid Crystalline Polymer Single-Chain Nanoparticles. *Polym. Chem.* **2017**, *8*, 3523−3529.
(28) Hou, X.; Guan, S.; Qu, T.; Wu, X.; Wang, D.; Chen, A.; Yang, Z. Light-Triggered Reversible Self-Engulfing of Janus Nanoparticles. *ACS Macro Lett.* **2018**, *7*, 1475−1479.
(29) Guan, S.; Deng, Z.; Huang, T.; Wen, W.; Zhao, Y.; Chen, A. Light-Triggered Reversible Slimming of Azobenzene-Containing Wormlike Nanoparticles Synthesized by Polymerization-Induced Self-Assembly for Nanofiltration Switches. *ACS Macro Lett.* **2019**, *8*, 460−465.
(30) Hooshmand, S. E.; Heidari, B.; Sedghi, R.; Varma, R. S. Recent Advances in the Suzuki−Miyaura Cross-Coupling Reaction Using Efficient Catalysts in Eco-Friendly Media. *Green Chem.* **2019**, *21*, 381−405.
(31) Ogba, O. M.; Warner, N. C.; O'Leary, D. J.; Grubbs, R. H. Recent Advances in Ruthenium-Based Olefin Metathesis. *Chem. Soc. Rev.* **2018**, *47*, 4510−4544.
(32) Duckett, S. B.; Newell, C. L.; Eisenberg, R. Observation of New Intermediates in Hydrogenation Catalyzed by Wilkinson's Catalyst, RhCl(PPh3)3, Using Parahydrogen-Induced Polarization. *J. Am. Chem. Soc.* **1994**, *116*, 10548−10556.
(33) Crabtree, R. H.; Mihelcic, J. M.; Quirk, J. M. Iridium Complexes in Alkane Dehydrogenation. *J. Am. Chem. Soc.* **1979**, *101*, 7738−7740.
(34) Dorel, R.; Echavarren, A. M. Gold(I)-Catalyzed Activation of Alkynes for the Construction of Molecular Complexity. *Chem. Rev.* **2015**, *115*, 9028−9072.
(35) Müller, T. E.; Hultzsch, K. C.; Yus, M.; Foubelo, F.; Tada, M. Hydroamination: Direct Addition of Amines to Alkenes and Alkynes. *Chem. Rev.* **2008**, *108*, 3795−3892.
(36) Mizushima, E.; Hayashi, T.; Tanaka, M. Au(I)-Catalyzed Highly Efficient Intermolecular Hydroamination of Alkynes. *Org. Lett.* **2003**, *5*, 3349−3352.
(37) Bohlen, J. L.; Kulendran, B.; Rothfuss, H.; Barner-Kowollik, C.; Roesky, P. W. Heterobimetallic Au(i)/Y(Iii) Single Chain Nanoparticles as Recyclable Homogenous Catalysts. *Polym. Chem.* **2021**, *12*, 4016−4021.
(38) Rothfuss, H.; Knöfel, N. D.; Roesky, P. W.; Barner-Kowollik, C. Single-Chain Nanoparticles as Catalytic Nanoreactors. *J. Am. Chem. Soc.* **2018**, *140*, 5875−5881.
(39) Moad, G.; Rizzardo, E.The History of Nitroxide-Mediated Polymerization. *Nitroxide Mediated Polymerization: From Fundamentals to Applications in Materials Science*; The Royal Society of Chemistry, 2015; Chapter 1, pp 1−44.
(40) Knie, C.; Utecht, M.; Zhao, F.; Kulla, H.; Kovalenko, S.; Brouwer, A. M.; Saalfrank, P.; Hecht, S.; Bléger, D. Ortho-Fluoroazobenzenes: Visible Light Switches with Very Long-Lived Z Isomers. *Chem.—Eur. J.* **2014**, *20*, 16492−16501.
(41) Hanlon, A. M.; Martin, I.; Bright, E. R.; Chouinard, J.; Rodriguez, K. J.; Patenotte, G. E.; Berda, E. B. Exploring Structural Effects in Single-Chain "Folding" Mediated by Intramolecular Thermal Diels−Alder Chemistry. *Polym. Chem.* **2017**, *8*, 5120−5128.
(42) Kovács, G.; Ujaque, G.; Lledós, A. The Reaction Mechanism of the Hydroamination of Alkenes Catalyzed by Gold(I)−Phosphine: The Role of the Counterion and the N-Nucleophile Substituents in the Proton-Transfer Step. *J. Am. Chem. Soc.* **2008**, *130*, 853−864.
(43) Merino, E.; Ribagorda, M. Control over Molecular Motion Using the Cis-Trans Photoisomerization of the Azo Group. *Beilstein J. Org. Chem.* **2012**, *8*, 1071−1090.
(44) Oscurato, S. L.; Salvatore, M.; Maddalena, P.; Ambrosio, A. From Nanoscopic to Macroscopic Photo-Driven Motion in Azobenzene-Containing Materials. *Nanophotonics* **2018**, *7*, 1387−1422.
(45) Beharry, A. A.; Woolley, G. A. Azobenzene Photoswitches for Biomolecules. *Chem. Soc. Rev.* **2011**, *40*, 4422−4437.